Surface-based observation of aerosol indirect effect in the Mid-Atlantic region

Fonya Nzeffe,[1] Everette Joseph,[1] and Qilong Min[2]

Received 18 September 2008; accepted 17 October 2008; published 29 November 2008.

[1] A method for assessing the aerosol indirect effect based on back trajectory analysis and cloud and aerosol properties derived from a combination of observations from the Multifilter Rotating Shadow Band Radiometer and microwave radiometer at a newly established atmospheric measurement field station in the Baltimore-Washington corridor is reported in this article. Six months of aerosol and cloud optical depth data are segregated according to air mass history based on back trajectory analysis. Under stagnant and polluted conditions where air flow across the region is predominantly from west–southwest, aerosol optical depth is on average three to four times greater than in air masses that advect rapidly from north and east. When sorted by mean cloud liquid water path, cloud-droplet effective radius in polluted air masses is on average 0.9 μm smaller than that observed under more pristine conditions. Analysis is presented to confirm the statistical significance of this result. **Citation:** Nzeffe, F., E. Joseph, and Q. Min (2008), Surface-based observation of aerosol indirect effect in the Mid-Atlantic region, *Geophys. Res. Lett.*, *35*, L22814, doi:10.1029/2008GL036064.

1. Introduction

[2] A number of researchers have applied space- and surface-based observations to study aerosol indirect effect (AIE). In accordance with *Twomey* [1974], these studies show that environments with high aerosol concentrations tend to produce brighter clouds by increasing cloud-droplet concentrations. *Han et al.* [1998] showed that high levels of cloud-droplet concentration occur frequently in regions with high production of cloud condensation nuclei (CCN), but that low cloud-droplet concentration occurs in regions with low CCN. Several recent studies have used surface-based observations of cloud and aerosol properties provided by the Atmospheric Radiation Measurement program (ARM) [*Ackerman and Stokes*, 2003] to offer more insight into AIE. For example, *Penner et al.* [2004] demonstrated the impact of AIE on radiative forcing using cloud and aerosol data from the ARM Southern Great Plains (SGP) and North Slope Alaska sites. *Kim et al.* [2003] demonstrated a proportional relationship between cloud optical depth (τ_c) and liquid water path (LWP), and an inverse relationship between the effective radius of these clouds and aerosol light scattering coefficient. *Feingold et al.* [2003, 2006] reported AIE based on aerosol-cloud interaction at cloud base using ARM data. Recently *Huang et al.* [2006] have shown significant reduction in effective particle diameter, optical depth and ice water path of ice cloud during dust storms over Northwestern China.

[3] Despite the important accomplishments of these and similar research, the uncertainties in estimates of the radiative forcing due to AIE on a global scale have not reduced [*Lohmann et al.*, 2007]. Significant progress to more precisely define global-scale radiative forcing due to AIE will require more long-term, high quality measurements across diverse climate regimes. Such data sets should enable better quantification of seasonal and interannual variability of aerosol direct and indirect effects.

[4] The present study reports results of AIE from data obtained over a period of six months (March–August 2005); at a newly established Howard University field station (39.054°N and 76.877°W) for atmospheric measurement in the Mid-Atlantic region. Analysis of radiation measurements, surface measurement of particulate matter (PM) at the site, and data from a nearby Aerosol Robotic Network (AERONET) [*Holben et al.*, 1998] show that this region experiences a wide range of inter and intra seasonal variability of aerosol loading: relatively low during winter months and frequent episodes of high loading during summer months. Studies suggest that a significant amount of aerosols observed in the region is transported from sources west of the region [*Li et al.*, 2005; *Environmental Protection Agency (EPA)*, 2004]. Aerosol loading is also controlled by the prevailing synoptic conditions particularly during summer months. In this study aerosol optical depths (AOD, hence forth τ_a) measured at the site are linked to the history of air masses, and meteorological conditions that influence the region. The effective radius of cloud-droplets that develop under air flow and meteorological conditions that are associated with high and low polluted episodes are investigated for signatures of AIE.

2. Measurements

[5] A wide range of sensors have been deployed at the Howard University Beltsville Campus (HB) facility in Beltsville, MD to observe atmospheric radiation, cloud properties, surface fluxes, and other climate and weather processes. Among these are a MultiFilter Rotating Shadowband Radiometer (MFRSR, henceforth MFR), a dual frequency (23.8 and 31.4 GHz) Radiometrics Water Vapor Radiometer (WVR-1100), a Total Sky Imager (TSI-880), a Ceilometer, a water vapor Raman LIDAR system, upward and downward viewing broadband sensors and a 31 m tower instrumented with standard meteorological sensors.

[1]Department of Physics and Astronomy, Howard University, Washington, D. C., USA.
[2]Atmospheric Sciences Research Center, State University of New York at Albany, Albany, New York, USA.

0094-8276/08/2008GL036064

The site is situated in a rural-suburban region between the Washington, DC and Baltimore, MD urban centers.

[6] Aerosol and cloud optical depths for the study are derived from measurements of the MRF. The MFR is a sensor with a shading band that rotates, measuring global downwelling irradiance with the band away from the diffuser, and diffuse irradiance when the band shades the diffuser from direct irradiance. It is calibrated using data acquired on clear sky days via the Langley analysis [*Harrison et al.*, 1994; *Harrison and Michalsky*, 1994]. The calibration constant $\mathbf{I}_0$ is used to compute transmittances during cloudy conditions [*Min and Harrison*, 1996].

[7] For quality control purposes, τ_a retrieved from the MRF at HB are compared with that from an AERONET site at NASA Goddard Space Flight Center (GSFC), approximately 5 miles southeast of the HB facility. For these comparisons, AERONET quality assured Level 2.0 τ_a data that have been cloud screened [*Smirnov et al.*, 2000] are used and interpolated to the 412 nm channel of the MFR using the Angstrom relationship. The correlation coefficient was found to exceed 0.98 which supports the overall reliability of the HB τ_a retrievals (Figure 1a). The results also suggest that spatial variability of τ_a between the two locations is relatively small for the cases considered. $PM_{2.5}$ ($PM \leq 2.5$ μm in diameter) data obtained from samplers operated by the Maryland Department of the Environment (MDE) at the site are also used in this study, to estimate aerosol loading under cloudy conditions. Although $PM_{2.5}$ was sampled only once every three days, $PM_{2.5}$ values correlated well with τ_a, yielding a correlation of 0.77. This result suggests that $PM_{2.5}$ can be used as a proxy for τ_a when τ_a retrieval is limited under cloudy conditions.

[8] Liquid water path is retrieved from sky brightness observations from the WVR using the so called "statistical method" by which the retrieval coefficients are derived from the climatology of radiosonde data for the site. The linear relationship between the brightness temperatures and the opacity is exploited to measure both the LWP and precipitable water vapor (PWV) [*Westwater et al.*, 2001]. The root mean square (rms) of clear sky biases was calculated to be 21 gm^{-2} for the six month period, but this value was not applied to correct the measured LWP values under cloudy conditions. Based on *Turner et al.* [2007] this error consists of instrument error, errors associated with the climatological profiles used for the retrieval (given day to day variability of atmospheric temperatures from this climatology), and errors from the absorption model used to develop parameters for the retrieval algorithm. The former two errors are considered random errors and thus are minimized with increasing sample size of data. The component of the error that derives from the absorption model is considered a systematic bias and moreover represents the preponderance of the total error [*Turner et al.*, 2007]. It is the relative difference of cloud-droplet effective radius (r_e) vs. LWP for clear and polluted conditions that is crucial to the approach put forth in this study for investigating AIE; the consequence of systematic biases is therefore minimized. The brightness temperature was used to screen the data so as to prevent contamination through precipitation and drizzle. From evaluation of 3 years of data acquired at HB, brightness temperatures above 100 K were always associated with precipitation. The LWP range considered in this paper did not exceed 200 gm^{-2} and thus well below the precipitation threshold of 300 gm^{-2}–400 gm^{-2} reported by *Gueldner and Spaenkuch* [1999]. The WVR is calibrated via the "Tipping curve" method [*Han and Westwater*, 2000; *Westwater et al.*, 2004] and a five minutes running-average is computed to smooth the data. Cloud-droplet effective radius is derived from measurement of diffuse irradiance from the MFR, and LWP of the WVR. Further details on the retrieval of r_e are given below in section 4.

3. Aerosol Loading and Air Mass History

[9] This study focuses on spring and summer of 2005 because aerosol background is significantly elevated from winter and there are more frequent episodes of low and enhanced loading. Using the HYbrid Single-Particle Lagrangian Integrated Trajectory (HYSPLIT) [*Draxler and Rolph*, 2003] model, back trajectories were conducted to segregate τ_a by air mass history observed at HB over the six month period. Trajectories were constructed for 48-hour periods at 5 levels (0.5, 1, 2, 3 and 4km above ground level), and several 48-hour trajectories were analyzed during the duration of each case. Cases with significantly divergent trajectories at multiple levels during the simulated period were not considered in order to minimize uncertainty regarding the source regions of the air masses. Cases of high aerosol loading tended to be associated with slow moving or stagnant air masses that flowed across the region from a westerly to southerly direction. Surface temperature and relative humidity (RH) were generally higher during episodes of high τ_a, as compared to low episodes. These conditions are typically associated with a well established ridge over the Eastern US and high pressure southwest of the region. Low aerosol loading was associated with northerly or easterly (marine) flow and relatively low temperatures and RH. The passage of cold fronts through the region or return flow from high pressure systems positioned offshore to the north east are synoptic cases that give rise to these conditions for low loading.

[10] Two cases of high aerosol loading and two cases of low aerosol loading that occurred during August 2005 are shown in Figure 1b as a sample of the many cases that are analyzed in the six-month data set. The time series of τ_a on day of year 229 and day 237 show values ranging from 0.1 to 0.3 and on day 217 and day 226 ranging from 1.0 to 1.7. 'Open diamond' represent AERONET data from GSFC while 'pluses' represent HB data. Trajectory analysis indicates that westerly air flow dominated the region on day 217 and day 226 (polluted case) in contrast to day 229 and day 237 (clean case) when northerly flow prevailed (Figures 1c and 1d).

4. Aerosol Indirect Effect

[11] During spring and summer of 2005, a total of 18 cloudy or partly cloudy days were identified with air mass histories that were consistent with high pollution episodes and 16 similar days with air masses that were consistent with moderate to good air quality conditions. Following *Min et al.* [2003] relatively uniform single-layer warm clouds lasting at least 30 minutes were the criteria used to select cloud cases for this study. Lidar observations of cloud

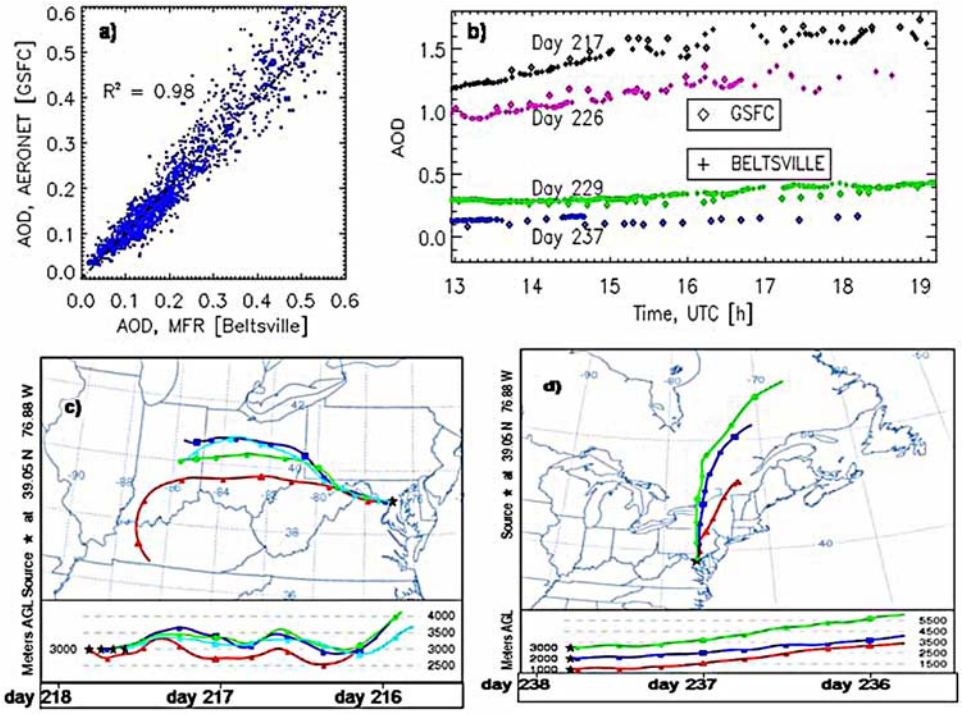

Figure 1. (a) The τ_a derived from the MFR (HB) vs. τ_a from AERONET (GSFC). (b) Time series of τ_a for polluted cases on day 217 and day 226 (top 2 pairs) and pristine cases on day 229 and day 237 (bottom 2 pairs). Open diamonds represent AERONET data while pluses represent τ_a values from HB. (c) HYSPLIT back trajectories at 3 km on day 217 (polluted case) are two hours apart and (d) trajectories for 1-, 2-, and 3 km on day 238 (clean case).

base heights, GOES satellite data of high cloud coverage, and cloud optical properties from the passive radiometers were all applied to determine if a particular case satisfied these criteria. Cloud based heights generally ranged from 2–5 km, and high cloud cases were rejected. In addition to air mass history a combination of $PM_{2.5}$ and τ_a observed during broken periods were also used to classify the cases as either polluted or clean. Polluted (clean) periods were associated with $PM_{2.5}$ values greater (less) than $\sim$ 10 $\mu g/m^3$ ($\sim$5 $\mu g/m^3$). These thresholds were based on the correlation of $PM_{2.5}$ with τ_a that was reported in section 2. Aerosol optical depth values less (greater) than 0.3 (0.5) were the criteria used to identify clean (polluted) periods when extended clear periods were present.

[12] Using an inversion algorithm developed by *Min and Harrison* [1996], τ_c and r_e of warm (water) clouds are obtained. The algorithm is based on a lookup table of transmittance at the 412 nm channel of the MFR to determine τ_c. Concurrent LWP and τ_c are applied to infer r_e base on a parameterization for cloud optical properties derived from Mie theory. Using this retrieval, *Min et al.* [2003] have shown that r_e values agree to within 5.5% with in situ measurements.

[13] To assess the impact of aerosol loading on cloud optical properties, r_e values are sorted into 6 bins of LWP with 20 gm^{-2} bin widths. Only LWP values ranging from 80 gm^{-2} to 200 gm^{-2} are considered since too few data points existed beyond 200 gm^{-2}, and estimates of droplet radius become poorer because of increased uncertainty in LWP below 80 gm^{-2}. The retrieval errors for LWP are estimated to be 20–30 gm^{-2}, and thus the uncertainty of r_e increases significantly for LWP values less than 80 gm^{-2} [*Marchand et al.*, 2003; *Turner et al.*, 2007].

[14] Cloud-droplet effective radius in this study ranged from 3–11 μm, which is consistent with values reported by other studies of continental clouds [*Marchand et al.*, 2003; *Sengupta et al.*, 2003]. The mean r_e values for each LWP bin are computed for high and low aerosol loading conditions and plotted against the arithmetic mean of each bin (Figure 2a). 'Squares' represent observations during polluted conditions, while 'asterisks' are observations under more pristine cases. Over the entire LWP range that is considered the mean r_e for cloud-droplets observed in air with high aerosol loading is less than that in air with low loading by as much as 0.9 μm. The plot indicates that droplet sizes increase with increasing LWP, but that the increase is greater for droplets in polluted air masses. Moreover r_e for polluted cases is smaller than that for cleaner conditions but that difference (r_e clean - r_e polluted) decreases by more than 50% across the range of LWP considered by this study. No systematic bias in cloud altitude between the clean and polluted clouds was observed in the 2–5 km range that was investigated. The results of a t-test analysis [e.g., *Wilks*, 1995] to assess the statistical significance of the mean r_e differences are presented in Figure 2a. For this calculation the mean and variance of r_e is determined for pristine and polluted cases for a given LWP bin. The binned clean and polluted r_e cases are treated as two independent samples because the data between the two samples were observed on different sets of days. Results of the t-test show that the difference in the mean re values for the polluted and pristine air masses is significant except for the last bin (Figure 2b). The analysis presented in Figure 2a was conducted for

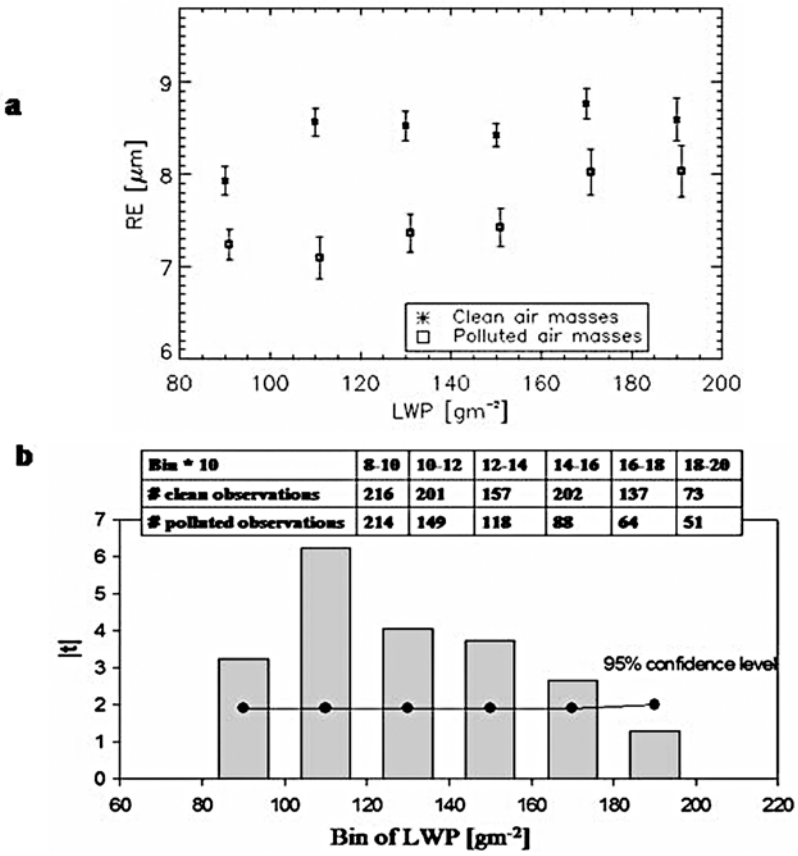

Figure 2. (a) Mean r_e vs. LWP. Squares represent r_e of clouds formed in polluted air masses and asterisks represent r_e of clouds formed in more pristine air masses. Error bars represent the standard errors of the mean. (b) T-test analysis of the mean values of r_e in Figure 2a shows a statistically significant difference except for the last bin. The table shows the number of observations in the respective bins.

5 minute averages, but the results of 15 minute and daily averaged cases do not differ sufficiently to alter the conclusions of the paper.

[15] Overall, these results are consistent with current understanding of cloud-droplet growth by condensation and collision. Cloud-droplets compete with each other as they grow through water diffusion. Under conditions of low LWP, higher CCN concentration increases competition among cloud-droplets and thus is a limiting factor on cloud-droplet radius or droplet growth. Competition is mitigated as LWP increases and the dominance of CCN concentration on cloud-droplet sizes is lessened. Also growth by collision may be enhanced for higher LWP.

5. Discussion and Conclusions

[16] Observations of aerosol and cloud optical properties derived from passive radiometric sensors deployed at a recently developed field site in Beltsville, Maryland are employed to investigate the impact of aerosols on cloud optical properties. Back trajectory analyses using the HYSPLIT model are applied to a six month period of aerosol observations, and results suggest that stagnant or slow moving air masses that flow from south and west of the region are more polluted than faster moving air masses from the north and east. This result is consistent with previous reports [*Li et al.*, 2005; *EPA*, 2004] that suggest that a significant amount of particulate matter observed over the eastern half of the United States is due to transport and is associated with industrial and biogenic sources. Analysis of $PM_{2.5}$ observation made at the site show that Sulfates and carbon compounds form the bulk of these aerosols during the warmer months of the year while Nitrates concentrations were only significant during the relatively colder months of the year from November through April; barely exceeding 3 $\mu g/m^3$.

[17] Analysis of cloudy cases with air mass histories that are consistent with high and low aerosol loading showed a reduction of the mean r_e for the former as compared to the latter. Mean cloud effective radius differed by 0.9 $m\mu$ for LWP values that ranged from 80 gm^{-2} to 200 gm^{-2}. This difference has been shown to be statistically significant for lower values of LWP. The result presented above is in accordance with the expectation of aerosol indirect effect as first introduced by *Twomey* [1974].

[18] Overall this study has demonstrated a reliable approach for assessing AIE based on cloud and aerosol optical properties derived from routine but high quality passive radiometric measurements. Acquiring these observations in the Mid-Atlantic corridor is particularly important because this region is often plagued by severe pollution episodes. While there has been many studies conducted to observe air pollutions processes in the region few have focused on the impact of aerosols on clouds or even more broadly the hydrological cycle. Long-term observations of cloud and

aerosol properties are required in diverse climate and air quality regimes to reduce the uncertainty of estimates of radiative forcing due to AIE. The data being collected at the HB site in Beltsville, MD combined with the approach reported here could potentially contribute to this effort.

[19] **Acknowledgments.** The authors gratefully acknowledge the National Oceanic and Atmospheric Administration (NOAA) Air Resources Laboratory (ARL) for the provision of the HYSPLIT transport and dispersion model and READY website (http://www.arl.noaa.gov/ready.html) used in this publication. Many thanks to the anonymous reviewers for their comments on the manuscript, Brent Holben and his staff for establishing and maintaining GSFC site as well as John Haus and the Maryland Department of the Environment for providing us with $PM_{2.5}$ data. This research was supported by a grant from NOAA EPP.

References

Ackerman, T. P., and G. M. Stokes (2003), The atmospheric radiation measurement program, *Phys. Today*, *56*, 38–44.

Draxler, R. R., and G. D. Rolph (2003), HYSPLIT-Hybrid Single-Particle Lagrangian Integrated Trajectory Model, http://www.arl.noaa.gov/ready/hysplit4.html, NOAA Air Resour. Lab., Silver Spring, Md.

Environmental Protection Agency (EPA) (2004), The particle pollution report: Current understanding of air quality and emissions through 2003, *EPA 454–R-04–002*, Washington, D. C.

Feingold, G., W. Eberhard, D. Veron, and M. Previdi (2003), First measurements of the Twomey indirect effect using ground-based remote sensors, *Geophys. Res. Lett.*, *30*(6), 1287, doi:10.1029/2002GL016633.

Feingold, G., R. Furrer, P. Pilewskie, L. A. Remer, Q. Min, and H. Jonsson (2006), Aerosol indirect effect studies at southern Great Plains during the May 2003 intensive operations period, *J. Geophys. Res.*, *111*, D05S14, doi:10.1029/2004JD005648.

Gueldner, J., and D. Spaenkuch (1999), Results of year-round remotely sensed integrated water vapor by ground-based microwave radiometry, *J. Appl. Meteorol.*, *38*, 981–988.

Han, Q., W. B. Rossow, J. Chou, and R. Welch (1998), Global survey of the relationships of cloud albedo and liquid water path with droplet size using ISCCP, *J. Clim.*, *11*, 1516–1528.

Han, Y., and E. R. Westwater (2000), Analysis and improvement of tipping calibration for ground-based microwave radiometers, *IEEE Trans. Geosci. Remote Sens.*, *38*, 1260–1276.

Harrison, L., and J. Michalsky (1994), Objective algorithms for the retrieval of optical depths from ground-based measurements, *Appl. Opt.*, *33*, 5126–5132.

Harrison, L., J. Michalsky, and J. Berndt (1994), Automated multifilter rotating shadow-band radiometer: An instrument for optical depth and radiation measurements, *Appl. Opt.*, *33*, 5118–5125.

Holben, B. N., et al. (1998), AERONET-A federated instrument network and data archive for aerosol characterization, *Remote Sens. Environ.*, *66*, 1–16.

Huang, J., P. Minnis, B. Lin, T. Wang, Y. Yi, Y. Hu, S. Sun-Mack, and K. Ayers (2006), Possible influences of Asian dust aerosols on cloud properties and radiative forcing observed from MODIS and CERES, *Geophys. Res. Lett.*, *33*, L06824, doi:10.1029/2005GL024724.

Kim, B., S. Schwartz, M. Miller, and Q. Min (2003), Effective radius of cloud droplets by ground-based remote sensing: Relationship to aerosol, *J. Geophys. Res.*, *108*(D23), 4740, doi:10.1029/2003JD003721.

Li, Q., D. J. Jacob, R. Park, Y. Wang, C. L. Heald, R. Hudman, R. M. Yantosca, R. V. Martin, and M. Evans (2005), North America pollution outflow and the trapping of convectively lifted pollution by upper-level anticyclone, *J. Geophys. Res.*, *110*, D10301, doi:10.1029/2004JD005039.

Lohmann, U., P. Stier, C. Hoose, S. Ferrachat, S. Kloster, E. Roeckner, and J. Zhang (2007), Cloud microphysics and aerosol indirect effects in the global climate model ECHAM5–HAM, *Atmos. Chem. Phys.*, *7*, 3425–3446.

Marchand, R., T. Ackerman, E. R. Westwater, S. A. Clough, K. Cady-Pereira, and J. C. Liljegren (2003), An assessment of microwave absorption models and retrievals of cloud liquid water using clear-sky data, *J. Geophys. Res.*, *108*(D24), 4773, doi:10.1029/2003JD003843.

Min, Q., and L. Harrison (1996), Cloud properties derived from surface MFRSR measurements and comparison with GOES results at the ARM SGP site, *Geophys. Res. Lett.*, *23*, 1641–1644.

Min, Q.-L., M. Duan, and R. Marchand (2003), Validation of surface retrieved cloud optical properties with in situ measurements at the Atmospheric Radiation Measurement Program (ARM) south Great Plains site, *J. Geophys. Res.*, *108*(D17), 4547, doi:10.1029/2003JD003385.

Penner, J., X. Dong, and Y. Chen (2004), Observational evidence of a change in radiative forcing due to the indirect aerosol effect, *Nature*, *427*, 231–234, doi:10.1038/nature02234.

Sengupta, M., E. E. Clothiaux, T. P. Ackerman, S. Kato, and Q. Min (2003), Importance of accurate liquid water path for estimation of solar radiation in warm boundary layer clouds: An observational study, *J. Clim.*, *16*, 2997–3009.

Smirnov, A., B. N. Holben, T. F. Eck, O. Dubovik, and I. Slutsker (2000), Cloud-screening and quality control algorithms for the AERONET database, *Remote Sens. Environ.*, *73*, 337–349.

Turner, D. D., et al. (2007), Thin liquid water clouds: Their importance and our challenge, *Bull. Am. Meteorol. Soc.*, *88*, 177–190.

Twomey, S. (1974), Pollution and the planetary albedo, *Atmos. Environ.*, *8*, 1251–1256.

Westwater, E. R., Y. Han, M. D. Shupe, and S. Y. Matrosov (2001), Analysis of integrated cloud liquid and precipitable water vapor retrievals from microwave radiometers during the Surface Heat Budget of the Arctic Ocean project, *J. Geophys. Res.*, *106*, 32,019–32,030.

Westwater, E. R., S. Crewell, and C. Maetzler (2004), A review of surface-based microwave and millimeter-wave radiometric remote sensing of the troposphere, *Radio Sci. Bull.*, *310*, 59–80.

Wilks, D. S. (1995), *Statistical Methods in the Atmospheric Sciences*, Academic, San Diego, Calif.

E. Joseph and F. Nzeffe, Department of Physics and Astronomy, Howard University, Washington, DC 20059, USA. (fnzeffe@yahoo.com)

Q. Min, Atmospheric Sciences Research Center, State University of New York, Albany, NY 12203, USA.